SLAC–PUB–7436
SCIPP 97/08
March 1997

Linear Electron-Electron Colliders*

Clemens A. Heusch

Institute for Particle Physics
University of California, Santa Cruz, CA 95064

Stanford Linear Accelerator Center
Stanford University, Stanford, CA 94309

Invited contribution to the Workshop on Future High-Energy Colliders,
Santa Barbara, CA, October 21-25, 1996.

*Work supported in part by Department of Energy contracts DE–AC03–76SF00515 and DE–FG03–92ER40689.

DISCLAIMER

Linear Electron–Electron Colliders

Clemens A. Heusch

Institute for Particle Physics
University of California, Santa Cruz, CA 95064

I INTRODUCTION

In the framework of the discussion on what shape our future machine arsenal should take so as to maximize our chances of penetrating beyond the realm where our astonishingly successful Standard Model of Particle Interactions holds undisputed sway, the present contribution is somewhat unusual: I am not here to convince our community to build yet another machine. Instead, my task is to convince you that in the established choices that we are headed towards, it is of great importance that the *Electron Collider* of the next generation, i.e., in the 0.5 to 1.5 TeV energy range, should be configured just such, as an *Electron* collider, *NOT* dedicated to just one incoming charge state (say, e^+e^-).

Now that we have exceeded the energy range that can be reached with circular/recirculating machines, we are freed from the need to have oppositely charged electrons as projectiles and targets. The colliding linac configuration sets no preferential condition on the chosen net charge; in fact, this is the first time we have a machine that may well serve to collide a variety of initial states at full energy $2E_B$ and luminosity (e^+e^+, e^+e^-, e^-e^-), or at slightly reduced center-of-mass energy, but still full luminosity (γ–e, γ–γ).

I will not belabor the case for initial states including high-energy photons *beyond* mentioning, in Section IV, the intimate connection that a successful realization of these collisions has with the availability of a high-quality e^-e^- facility. Rather, I will attempt to show, briefly, that there is little if any problem in configuring an Electron Collider such that it can be run in either charge mode with comparable performance characteristics, excepting only the polarization parameter; and I will proceed to show you the very rich physics potential of the e^-e^- collision mode—some of it unique, some complementary to the promise of the more thoroughly discussed e^+e^- collision mode.

Before embarking on this enterprise, it is fair to remind you that the first electron collider was, in fact, built for the explicit purpose of testing the limits of precision to which the Standard Model of the 1950s, Quantum Electrodynamics, could be shown to follow its theoretically accepted pattern: Barber,

Gittelman, O'Neill, and Richter built their e^-e^- circular collider, with two rings, on the Stanford Campus, and were able to reach center-of-mass energies of 1012 MeV, at which they tested Møller scattering for possible cutoff or form factor effects. The first step toward testing the broader, emerging Standard Model that included the strong and weak interactions, showed the virtues of using e^+e^- annihilation, and led to the immensely successful operation of a slew of storage rings that would teach us a large fraction of our present state of knowledge, was initiated in Frascati by Bruno Touschek with his ADA ring [1]. Today's running of LEPII is, beyond any doubt, the last hurrah of the circular e^+e^- machines—and it would be disingenuous to suggest installation of a second ring in its tunnel for the purpose of running e^-e^- experiments.

Fortunately, the Linear Electron Colliders, the NLC version of which is described in detail in these proceedings, have no problem worth mentioning being configured in the e^-e^- (or, should that be of separate interest, the e^+e^+ initial state).

II MACHINE CONSIDERATIONS

Linear acceleration of electrons and positrons is identical once the phase difference with regard to the RF field is taken into account. What is not identical is the emittance of the beams entering the linac structure, and, as a result, the potential phase space effects due to wake fields building up in the accelerating structure. More differentiation needs to be considered for the interaction of the accelerated beams at the interaction point: the luminosity that can be reached with oppositely charged beams is enhanced by the electrostatic attraction of the two beams ("pinch effect"); conversely, like-charge beams repel each other and "blow up" the interaction area ("anti-pinch"). Also, there is the need for different handling of the "spent" beams beyond the interaction point—particularly in the case of non-zero crossing angle: like-sign beams need more attention because they do not automatically follow the optical path of the oppositely moving antiparticle, up to ejection into a beam dump. While all of these points are basically amenable to given technical solutions, there is one qualitative difference that cannot be made up for in any known way: electron guns can easily reach high degrees of polarization for the emerging e^- beams, and we do not believe there is any relevant limitation as to the available intensity. 80% polarized electrons are routinely used at SLAC, and there is no reason to believe that this value cannot be raised to above 90% in the intermediate time frame. It turns out that this capability is of immense value for the enhancement of a number of Beyond-the-Standard-Model effects, and for the suppression of backgrounds, as we will see below. For positron beams, there is strictly no way to reach similarly high polarization values; a number of schemes are being tested, but there is no hope of reaching anything

beyond about 60%—which is not sufficient for precision work in a number of connotations.

Fairly detailed studies of the generalized luminosities $\mathcal{L}$ in terms of incident Gaussian bunches were made by J. E. Spencer [2]. He points out that while it would be nice to put the full current available from the gun, per RF pulse of the linac, into a single bunch for acceleration, this would be highly undesirable for reasons of emittance growth, energy spread, and beamstrahlen intensities. Rather, he plays a number of scenarios with multi-bunch operation ($n_B > 1$) and f_T, the number of bunch trains per second (which is the same as the RF rep rate). With N_B the number of electrons per bunch and a luminosity enhancement (or disruption) factor H_D, the luminosity can be expressed as

$$\mathcal{L} = \frac{f_T n_B N_B^2 H_D}{4\pi\sigma_z^*\sigma_y^*}\zeta \rightarrow \frac{f_T n_B N_B^2 \gamma H_D}{4\pi\epsilon_n\beta^*}\zeta = \frac{f_T n_B N_B^2 \gamma}{4\pi\hat{\sigma}^2}\zeta \propto \frac{P_b}{\hat{\sigma}^2}\left(\frac{\hat{N}_b^2}{N_b}\right). \qquad (1)$$

Here, ζ is an efficiency factor which may well approach 1, and the σ are geometrical transverse spot sizes. Multibunch trains of $n_B = 100$ will help to distribute the total charge per RF pulse more evenly down the linac structure, which may well help to make electron currents easier to raise than positron currents that are injected into the linac from cooling rings. Many practical problems have to be addressed—the multibunch operation will necessitate a crab-crossing interaction geometry, and overall luminosity optimization may well make a plasma lens advisable for the compensation of the electrostatic beam-beam repulsion [3]—but overall there is an expectation that the implementation of a highly stable e^-e^- operation of the Next Linear Collider will have little trouble coming in with luminosities commensurate with what an e^+e^- version of the same machine can do.

Given the high demands on instrumentation that will be needed to produce efficient photon beams from laser photons backscattered within less than 1 cm of the IR off the incident electron beams, it will be very unwise to couple e^-e^- experimentation *a priori* with e–γ and/or $\gamma\gamma$ operation. Rather, the urgency of the physics program that can fruitfully be addressed by the e^-e^- mode argues powerfully for the implementation of the electron–electron version early on, at turn-on time of the colliding linacs. The physics motivations that will have to decide on the appropriate initial-state choice therefore are our paramount interest.

III PHYSICS PROMISE

In discussing the motivations for implementing the electron-electron version of the Next Linear Collider (or its equivalent), we will follow roughly the 1996 Snowmass Study organization. In an attempt to highlight both the uniqueness of the goals that lend themselves to experimental investigation from an e^-e^-

initial state and the complementarity of the different approaches, we will treat a few problems in more detail than others; this will serve to illustrate the strengths of this channel, but does not imply a lack of interest in the studies more cursorily advanced below. We hope to rectify any such impression by the concluding compilation of which physics problem will be accessible to which type of experimental approach.

A Weak Electroweak Symmetry Breaking: Higgs Bosons

Whether the LHC and/or the Tevatron manage to find credible evidence for Higgs boson production, it is almost certain that the Electron Collider will play a pivotal role in the investigation of the Higgs sector of electroweak symmetry breaking (EWSB). The much-touted discovery channel for the e^+e^- version of our collider is via the "Higgs radiation" graph of e^+e^- annihilation into a virtual Z boson [Fig. 1(a)]. While this graph provides a good signature (particularly for the fraction where the Z decays into muon pairs) and a sizeable cross-section close to threshold, its production rate drops with $1/s$. At higher energies, WW fusion and ZZ fusion [Fig. 1(b)] take over; but while the first of these has a factor of ten cross-section advantage over the latter, the undetectable neutrinos in the final state much decrease the discovery potential of this process, whereas the latter has the advantage of furnishing us with the scattered electron-positron pair for final-state reconstruction.

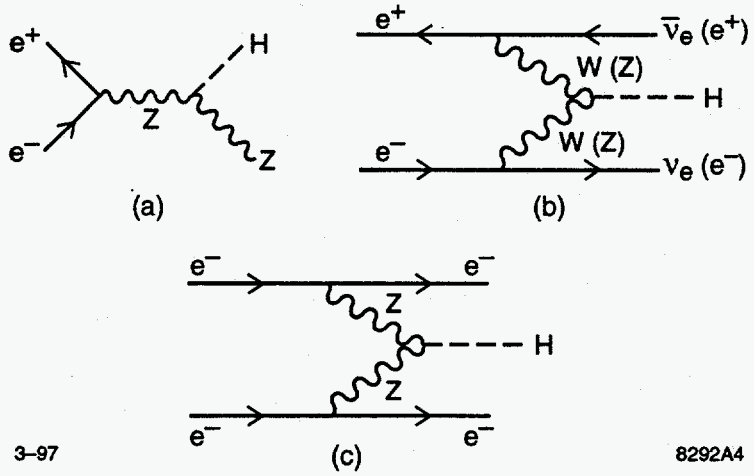

FIGURE 1. (a) "Higgs radiation": e^+e^- annihilation into a virtual Z boson followed by "Higgsstrahlung"; (b) WW fusion and ZZ fusion in e^+e^- collisions; (c) central production of Higgs boson in e^-e^- collisions. H^0 mass can be reconstructed if outgoing electron momenta are measured.

This is where the e^-e^- initial state takes over [Fig. 1(c)]: like-sign electron pairs are a rare background product, so that, for the kinematic region $\sqrt{s} > 2.5\, m_H$, the process $e^-e^- \to e^-e^-H$ provides the favored discovery and study channel. In a recent paper, Minkowski [4] investigated the usefulness of this method for a detailed study of Higgs boson production and decay by means of a good measurement of the tagged electron angles and energies: the central mass is well resolved by

$$M^2_{rec} = (p_{rec})^2; \tag{2}$$

its decay can be subsequently determined.

This procedure has several signal advantages:

a. In contrast to the Higgsstrahlung graph (in e^+e^- annihilation), the ZZ fusion cross-section saturates above the threshold region; it becomes proportional to m_Z^2, and it does not depend much on the scalar mass as long as this is well below the center-of-mass energy at which the measurement is being performed.

b. Once our detector imposes an angular cut (say, of a five degree cone in the forward and backward directions), the cross-section becomes geometric and decreases as s^{-1} (cf. Fig. 2), but remains roughly independent of the scalar mass.

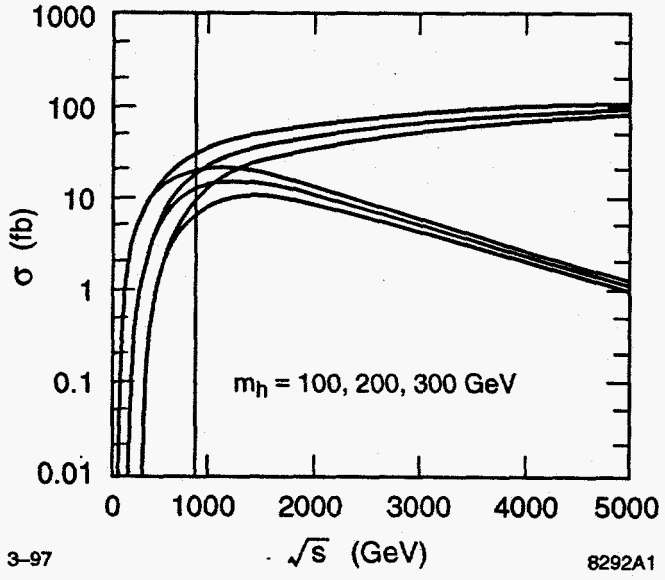

FIGURE 2. Cross-section for production of a standard scalar as a function of c.m. energy with and without angular cut (upper curves), for given H masses. Incoming electrons are pure left-handed.

c. There is essentially no influence on the event rates (shown, for typical parameters, in Fig. 3) due to the helicities of incoming electrons. Since the principal background is W^+W^- pair production via $\gamma\gamma$, and to a much reduced degree, ZZ fusion according to

$$e^-e^- \to e^-e^-W^+W^-, \tag{3}$$

the detector-imposed small-angle cut serves to diminish the background signal by virtue of the fact that many of the final-state electrons will exit at smaller angles.

d. The central mass thus studied may well decay "invisibly"—say, into gluino pairs—and it will not detract from our discovery potential; this is indicated in the mass plot shown in Fig. 4: the mass peak is strictly due to the final electrons' kinematics, while the background is due to added W pair production.

Obviously, this measurement is applicable to all CP-even scalars, such as either the basic H boson or its MSSM (minimal supersymmetric) cousin h; it changes only in angular distribution for the CP-odd A boson. If the LHC or the Tevatron discover any of these, our process may well help define the optimal running energy of an NLC, for a detailed and clean investigation of Higgs boson properties.

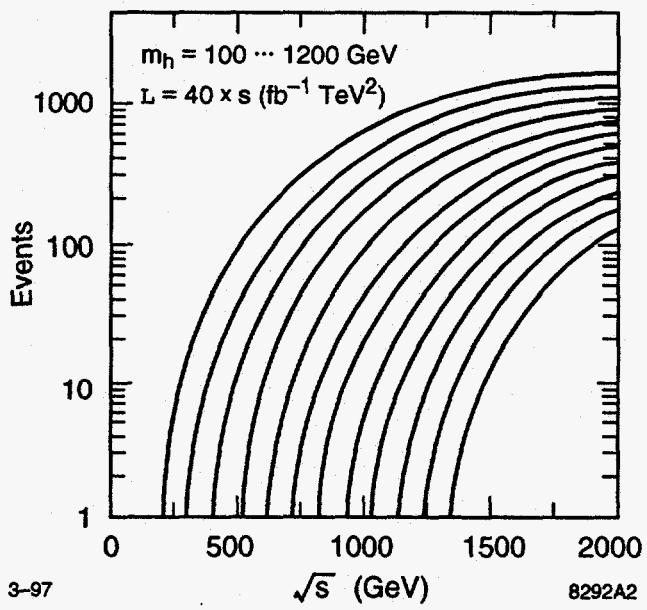

FIGURE 3. Event rates for production of neutral Higgs bosons by ZZ fusion from left-handed e^-e^- interactions, for given luminosity.

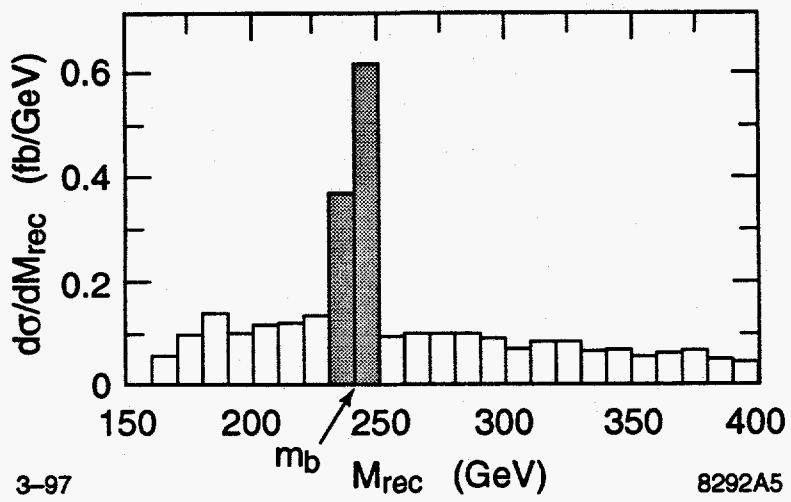

FIGURE 4. Differential cross-section for production of a 240 GeV/c^2 H^0 scalar at $\sqrt{s} = 850$ GeV, together with background due to the reaction $e^-e^- \to e^-e^-W^+W^-$. An angular cut between incoming and outgoing electrons is needed for recoil mass definition and background reduction.

B Extended Higgs Sector

Whereas neutral Higgs boson production will occur in minimal or extended models of mass generation, so that its observation will not *eo ipso* give definitive answers to the scenario in which they make their appearance, singly or doubly charged scalars are more specific to the models which contain them as telling components. Clearly, charge, helicity, and weak hypercharge conservation permit the e^-e^- initial state with adjustable helicities to fathom a broad class of extended models.

In the simplest tree-level realization of such extensions—most familiar to us from the MSSM framework—there is a minimal two-Higgs-doublet scenario. It lends itself to a detailed study by means of the reaction

$$e_L^-e_L^- \to W^-W^-\nu_e\nu_e \; (W^-W^- \to H^-H^-), \tag{4}$$

with two negative W bosons scattering into two negative Higgs bosons, and missing momentum taking the place of the unobserved neutrinos in the final state (cf. Fig. 5). Rizzo [5] studied this process in some detail and points out that, while the bare tree-level MSSM H^-H^- production cross-section is probably below detection level at an NLC, radiative corrections will raise the cross-section dramatically. Once we go beyond a basic two-doublet model, it may take some care to remain within the bounds of the $\rho = 1$ condition, but there are credible choices that add various basic triplet scalars (for a relatively simple version, see Ref. [6]). Spontaneous symmetry breaking within a custodial SU(2) framework leads to physical $\underset{\sim}{5}$ and $\underset{\sim}{3}$ scalar representations

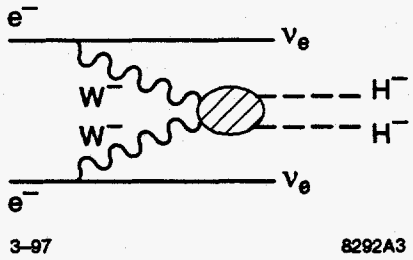

FIGURE 5. WW fusion graph for H^- pair production.

with singly and doubly charged Higgs bosons. Depending on parameter choices that include a possible resonance structure if the quintuplet mass is more than twice that of the triplets, such scenarios may well lead to wide variations in the resulting cross-sections, up to values in the 100 fb region.

Gunion [7] devoted a special study to the chances of discovering doubly charged Higgs bosons in e^-e^- scattering: given that we have no clear idea on the presumptive coupling strength c_{ee} for direct $H^{--}e^-e^-$ coupling [Fig. 6(b)], we have to resort to H^{--} production via W^-W^- fusion [shown in Fig. 6(a)]—which occurs to the tune of a full unit of R (the QED width for $e^+e^- \to \mu^+\mu^-$ at given energy), illustrated for various m_H values in Fig. 7. The H^{--} states may decay via W^-H^-, adding special spice to this field of inquiry.

Given that any putative effect can immediately be killed by appropriate manipulation of the incoming helicity, it becomes obvious that an electron-electron collider provides the ideal laboratory for the investigation of a large set of extended Higgs sector scenarios.

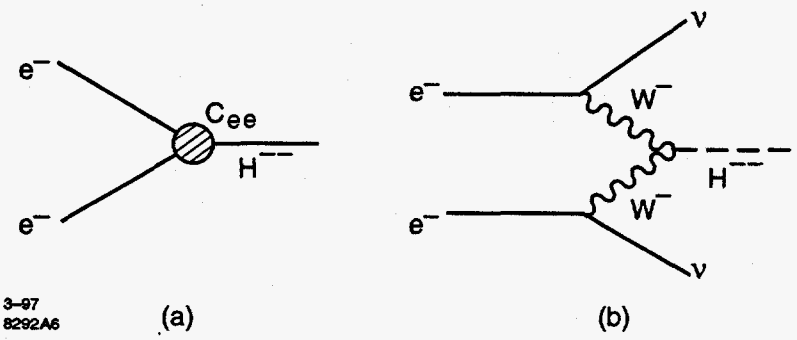

FIGURE 6. (a) Direct production of H^{--} from an e^- pair, with unknown coupling c_{ee}, and (b) WW fusion graph for H^{--} production.

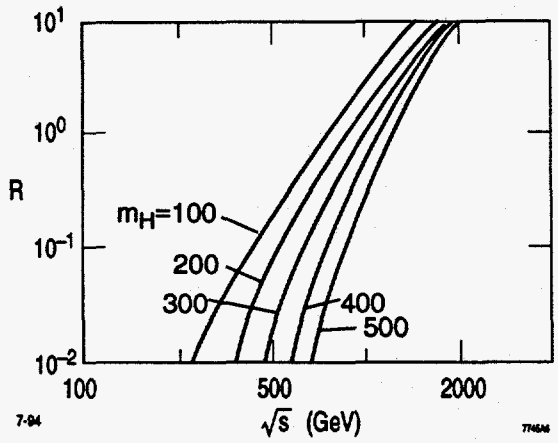

FIGURE 7. Production cross sections, by an NLC/TLC e^-e^- collider, of doubly charged H^{--} bosons in the mass range from 100 to 500 GeV/c^2, in units of R.

C Supersymmetry

In the coming years, the frenzied search for Supersymmetry signals will doubtlessly continue at LEPII and at the Tevatron. But it can confidently be anticipated that we will need higher-energy electron colliders for dedicated and focused studies of many relevant SUSY parameters—even though the first discoveries may well precede their turn-on. A detailed investigation of the sparticle mass spectrum, of decay distributions, and of all the relevant couplings will be much helped by the tight control we have over the energy and polarization of our incident beams. The electron-electron mode, simply by dint of its easily controlled helicities, is particularly suited to do selectron searches, to measure neutralino masses, and to determine the most important U(1) and SU(2) couplings.

The first of these concerns is well-illustrated in a study by Cuypers *et al.* [7], who studied the production of selectron pairs and chargino pairs in electron-electron collisions as in Figs. 8(a) and 8(b). As Peskin points out in his SUSY lecture notes [8], the preferential coupling of e_R^- to the selectron causes production cross-sections to be widely different (by three orders of magnitude) for the RR vs LL incoming helicity combinations, as shown in Fig. 9. That, in turn, has the considerable advantage of decoupling the right-handed incoming electrons, preferred for selectron pair production, from the W^- emitted in the lowest-order background graphs. The principal remaining background process in the final state e^-e^- plus missing transverse momentum (from unobserved neutralinos) would be due to the reaction

$$e^-e^- \to e^-e^-Z^0(Z^0 \to \nu\bar{\nu}). \tag{5}$$

It can fairly be excluded through judicious electron energy cuts, as indicated in Fig. 10(b). A purely kinematical evaluation of this plot can also yield a

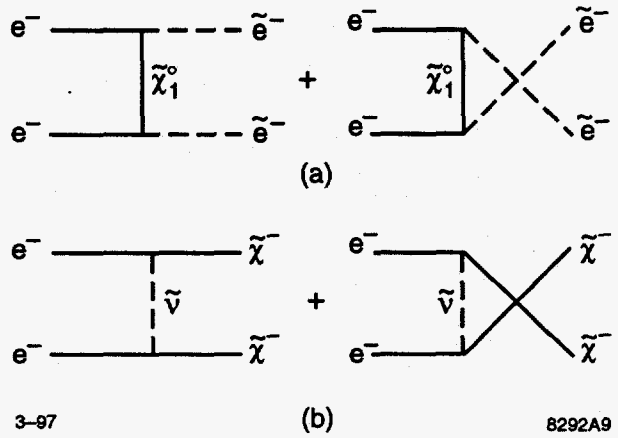

FIGURE 8. (a) $\tilde{e}$ pair production from e^-e^- collisions by $\tilde{\chi}_0$ exchange. (b) Like-sign $\tilde{\chi}^-$ pair production by $\tilde{\nu}$ exchange.

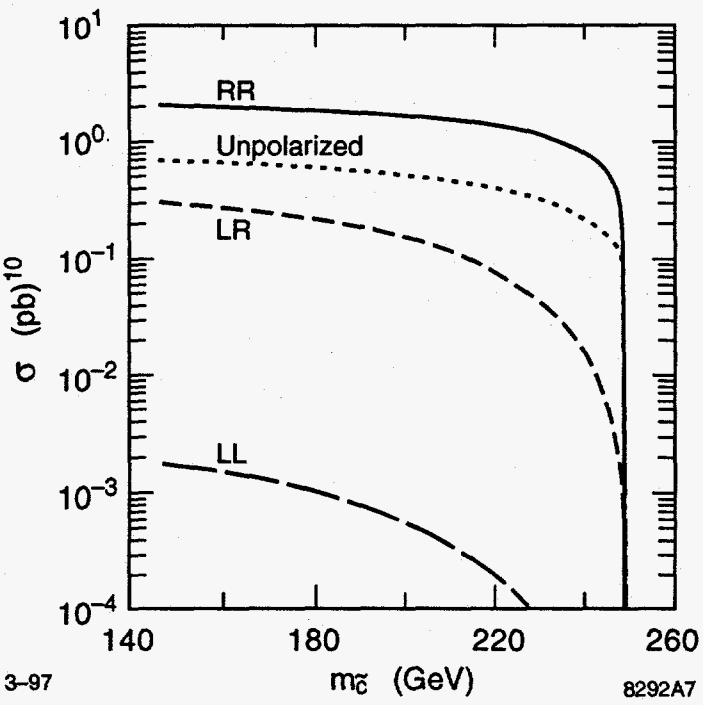

FIGURE 9. Cross-section for $\tilde{e}^-$ pair production from e^-e^- collisions as a function of $\tilde{e}$ mass, for an e^-e^- collider of $\sqrt{s} = 500$ GeV, with the incident electron helicities as indicated. For SUSY parameters see Ref. [7].

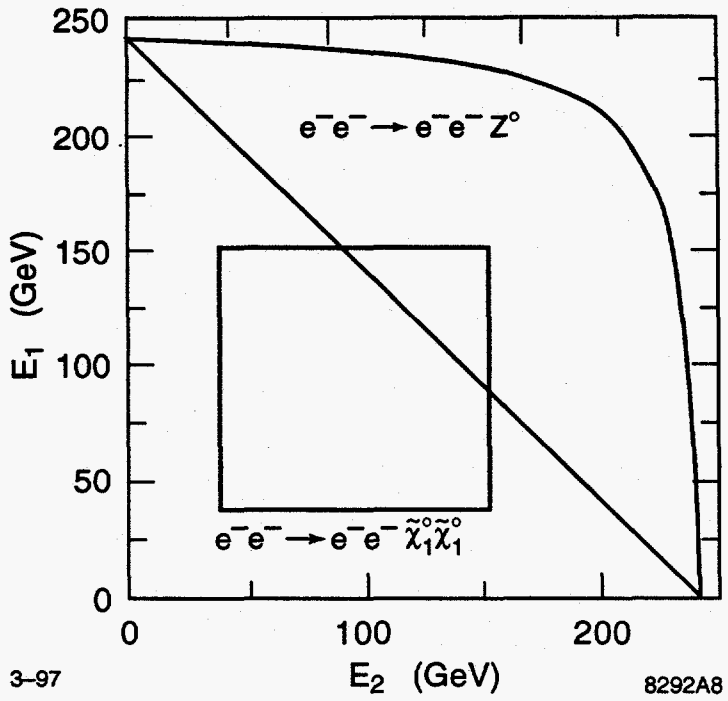

FIGURE 10. Permitted energy range for the two electrons observed in the two reactions mentioned in the figure. For $\tilde{e}$ decay, we assumed $m(\tilde{e}) = 200$ GeV, $m_{\tilde{\chi}^0} = 100$ GeV. The diagonal cut eliminates the background while losing little signal.

direct measurement of the masses both of the selectron and of the lightest neutralino.

The chargino pair production process (Fig. 8(b)) profits even more from the well-defined helicity content of the initial state: charginos couple only to left-handed leptons, so that only the LL combination will contribute. The fact that their masses as well as their couplings to selectrons (in the decay channel that leaves only a neutrino unobserved) are functions of the three SUSY parameters $\tan\beta$, μ, and M_2, further enhances the status of a clean search as an agent for a fuller exploration of our most elegant candidate for an extension of the Standard Model.

In the same vein, it is important to notice that for the case where the higgsino is the lightest SUSY particle, the masses of neutralino and chargino are closely spaced; this makes the like-sign selectron pair production process, the background of which is depressed by about an order of magnitude below the e^+e^- case, particularly significant.

D Strong EWSB: Strong WW Scattering

It is well-understood that, should we not find an elementary Higgs boson well below the TeV level, the Higgs mechanism will have to be impersonated

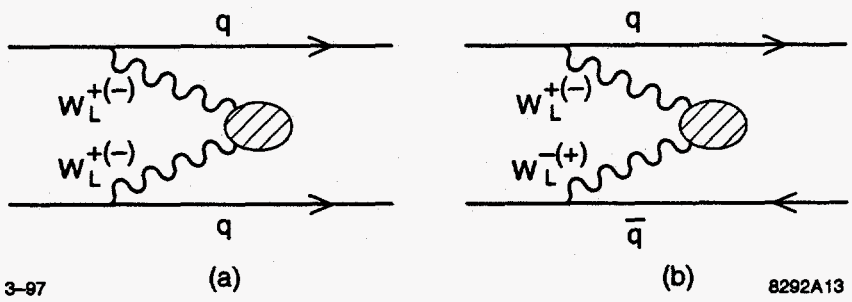

FIGURE 11. Strong WW scattering from (a) quarks in hadron collisions and (b) quarks-antiquarks in hadron collisions.

by a new strong interaction of longitudinal W bosons—dubbed the Fifth Force by M. Chanowitz [9]. This will lead to an entire field of new dynamics that will have to be fully explored—as basic in the TeV region as $\pi\pi$ scattering was below 1 GeV. This cannot possibly be exhausted at e^+e^- colliders, which are limited to the $J = 0, 1$; $I = 0, 1$ channels. The (possibly very distinctive) $I = 2$ channel can be uniquely well investigated in the e^-e^- collider at its upper energy reach, by means of the process

$$e^-e^- \to W^-W^-\nu\nu,\ W^-W^- \to \ell^-\ell^-\nu\nu. \tag{6}$$

Whereas hadron colliders in the TeV region will produce signals due to strong W_LW_L scattering according to Figs. 11(a) and 11(b), these will be hard to separate from the expected backgrounds: the worst of these is tree-level

$$qq \to q'q'\ W^+W^+(\text{or } W^-W^-), \tag{7}$$

visible in terms of the final states $\ell^+\ell^+$, (or $\ell^-\ell^-$) plus missing transverse momentum. Essentially all of the relevant W's are transverse, and effects of strong WW scattering will be very hard to isolate. The situation is more favorable in the e^-e^- initial state (Fig. 12), where the high polarization we can achieve for both incoming channels enhances the cross-section by a factor of four: any observable signal can therefore be strengthened by a set of judicious cuts [10,11]. If we are really lucky, it may well stick out prominently in the shape of a resonant scalar or vector state in the reconstructed WW or bb mass distributions. An example is shown in Fig. 13—which illustrates simultaneously the effect of an extended Higgs sector (cf. Fig. 6).

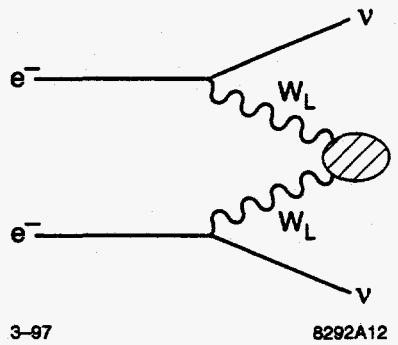

FIGURE 12. Strong $W_L W_L$ scattering in $e^- e^-$ collisions. This will work only for left-handed electrons.

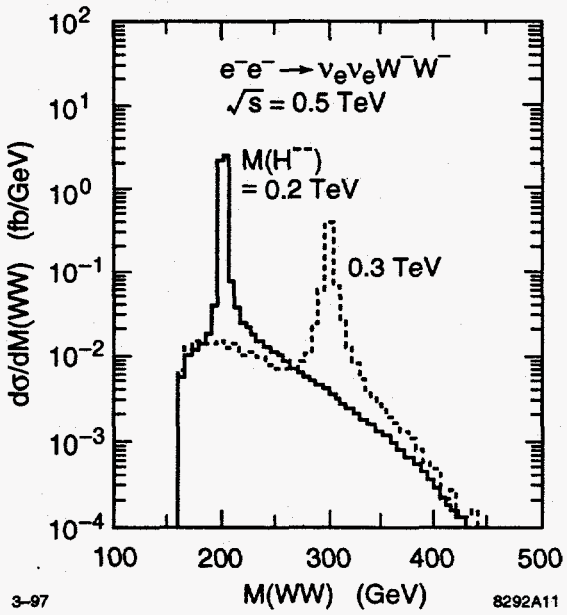

FIGURE 13. Distribution in the $W^- W^-$ invariant mass for $e^- e^- \to \nu_e \nu_e W^- W^-$, including the contribution of a doubly-charged Higgs boson of mass $M(H^{--}) = 0.2$ or 0.3 TeV.

E Anomalous Gauge Couplings

One particular manifestation of an extended gauge group structure is the deviation of trilinear and/or quartic couplings from the Standard Model values. For the first set of these non-Abelian couplings, the relevant Lagrangean L_{eff}^{WWV} (see, e.g., Ref. [12]) contains the SM-specified coupling parameters

$$\begin{aligned} g_\gamma &= e & g'_\gamma &= 1 \\ g_Z &= e\cot\theta_W & g'_Z &= 1 \\ \\ k_\gamma &= 1 & \lambda_\gamma &= 0 \\ k_Z &= 1 & \lambda_Z &= 0, \end{aligned} \tag{8}$$

where electromagnetic gauge invariance fixes $g_\gamma^1 = 1$. To do a thorough investigation of all possible deviations, the Electron Collider should be used in all its charge modes for complementary information. In particular, the radiative corrections are quite different in the e^-e^- case, and should lead to added valuable information.

TABLE 1. A sampling of processes and associated gauge boson couplings measurable at e^-e^- colliders.

Process	Couplings probed
$e^-e^- \to e^-\nu W^-$	$WW\gamma$, WWZ
$e^-e^- \to e^-e^-Z$	$ZZ\gamma$, $Z\gamma\gamma$
$e^-e^- \to e^-\nu W^-\gamma$	$WW\gamma$, WWZ
$e^-e^- \to \nu\nu W^-W^-$	$WWWW$
$e^-e^- \to e^-\nu W^-Z$	$WWZZ$
$e^-e^- \to e^-e^-ZZ$	$ZZZZ$

The fact that the polarization of the incoming electron beams can easily be reversed, again makes the e^-e^- channel particularly useful, as the plots of the total cross-section sensitivity, for the process $e^-e^- \to e^-\nu W^-$, to small changes in the various indicated parameters illustrated in Figs. 14(a) and 14(b). Table 1 shows to which triple or quartic couplings individual e^-e^- reactions are sensitive; and Table 2 gives a comparison of the parameter space that is open to investigation by a 0.5 TeV Electron Collider with presently available coupling parameter limits. This comparison speaks for itself, but should be complemented by the capabilities of other incoming charge states.

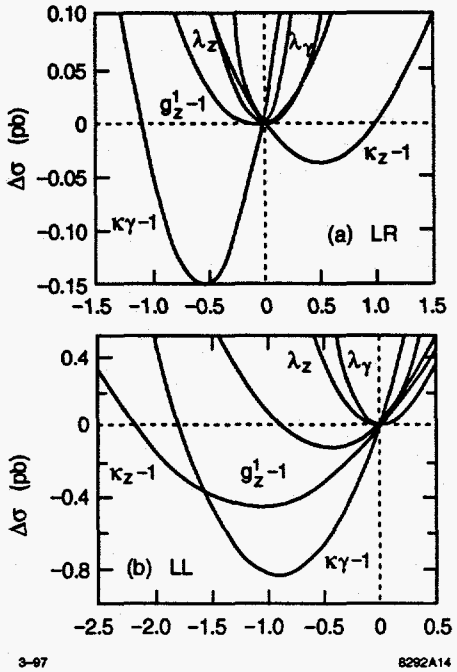

FIGURE 14. Contribution to the total cross section of each of the anomalous couplings, while all others are held to their Standard Model values, (a) for LR incoming electron helicities, (b) same, but for *LL*. The Standard Model cross sections are 3.19 *pb* for *LL* polarization and 0.348 *pb* for *LR*.

TABLE 2. Parameter values which can be tested by a particular experiment at 90% CL. The boldfaced numbers correspond to limits already set. For the generic 500 GeV linear collider LC500, we have assumed an integrated luminosity of 10 fb^{-1} for electron or photon beams. For the e^-e^- option we have used the combined information from *LL* and *LR* beam polarizations.

Machine/Experiment	g_z^1		K_γ		K_Z		λ_γ		λ_γ	
	min	max	min	max	min	max	min	max	min	max
UA2			-3.1	4.2			-3.6	3.5		
Tevatron			-2.4	3.7						
HERA			0.5	1.5			-2	2		
Tevatron			0.5	1.8	0.2		-0.2	0.2	-0.4	0.4
LHC			0.8	1.2	0.8		-0.02	0.02	-0.03	0.03
LEPII			0.86	1.87	0.76		-0.4	0.4	-0.4	0.4
LC500 e^+e^-			0.985	1.14			-0.02	0.04		
LC500 $e^+\gamma$			0.96	1.04			-0.05	0.05		
LC500 $\gamma\gamma$			0.98	1.015			-0.04	0.075		
LC500 e^-e^-	0.91	1.07	0.985	1.015	0.96	1.04	-0.045	0.075	-0.11	0.06

F Compositeness

As we are about to enter yet another energy regime of "point-like" particle interactions, it is only natural that we ask for the reach which this regime holds with respect to a potential energy scale where the "next layer of composite structure" might peel off. Møller scattering, it turns out, is more sensitive to the appearance of a new compositeness scale than Bhabha scattering, due to crossing term cancellations in the cross-section calculations. T. Barklow [13] investigated this issue in terms of a $1/\Lambda$ expansion of the relevant effective Lagrangean density operator, where the relevant four-fermion operators are written in terms of pure helicity fields.

By measuring the angular distribution of Møller scattering over the angular range $|\cos\theta| < 0.9$, 95% CL fits to the expected shape result in the sensitivities shown, assuming an integrated luminosity of 680 $pb^{-1} s/M_Z^2$ (for an easy comparison with existing PETRA limits), in Figs. 15 and 16. The first of these compares Bhabha with Møller scattering without giving the latter the benefit of polarization; clearly, e^-e^- must be the channel of choice at the energies covered in this plot. When we make the transition to polarized electrons, Møller scattering, at energies up to 1 TeV, is shown (Fig. 16) to be superior by a considerable stretch, reaching well beyond 150 TeV in its substructure sensitivity—obviously a highly topical capability of the TeV Electron Collider.

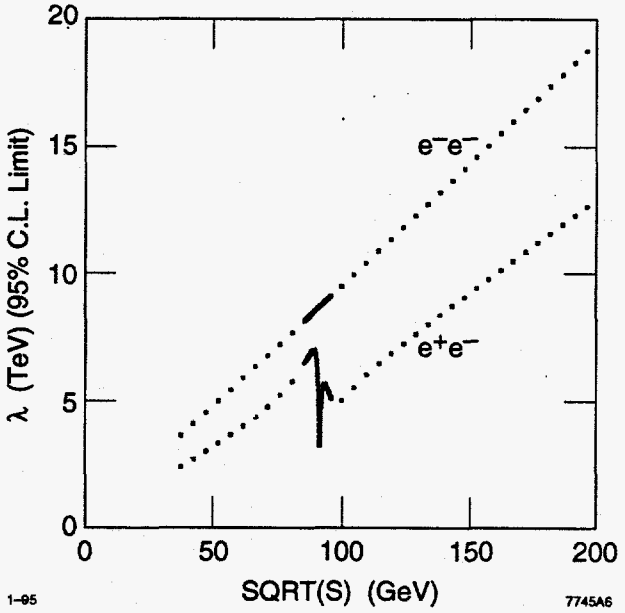

FIGURE 15. The 95% CL limits that can be obtained for the compositeness scale Λ_{LL} as a function of the e^-e^- or e^+e^- center-of-mass energy. The luminosity is given by $\mathcal{L} = 680\ pb^{-1} \times s/M_Z^2$. The beams are assumed to be unpolarized.

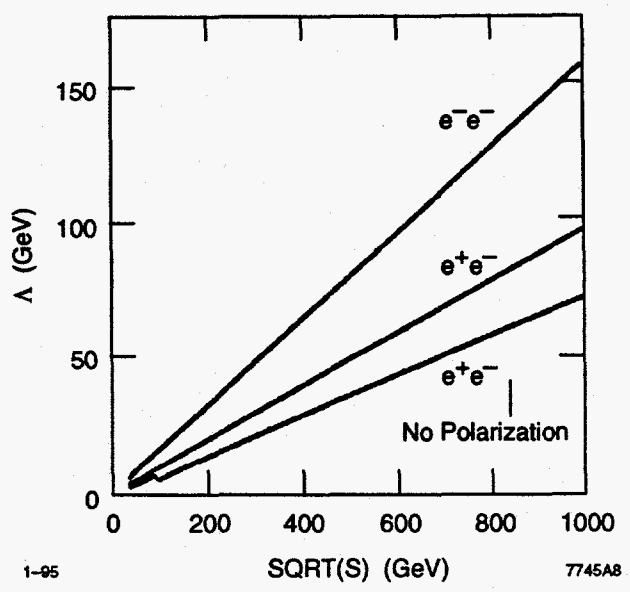

FIGURE 16. The 95% CL limits that can be obtained for the compositeness scale Λ_{LL} as a function of the e^-e^- or e^+e^- center-of-mass energy. The luminosity is given by $\mathcal{L} = 680\ pb^{-1} \times s/M_Z^2$. The polarization of the electron beam(s) is indicated in the figure.

G New Gauge Bosons: Z', Dileptons

Another standard quest, as we widen our kinematic parameter space, is the search for new gauge bosons—heavier Z' with either standard or exotic couplings, but potentially also more exotic bosons that might show up as s-channel structure in e^-e^- collisions.

The exchange of heavier Z' bosons in e^+e^- and e^-e^- scattering has been investigated in a sequential Standard Model, in LR-symmetric models, and in broader classes of models [14] – [16]. We limit ourselves to show, in Fig. 17, how sensitive Møller scattering is in comparison to Bhabha scattering when it comes to resolving the coupling parameters $v_{Z'}$, $a_{Z'}$ which enter into the cross-sections, at 95% CL, for a Z' mass of 2 TeV, and an Electron Collider energy of 0.5 TeV. For $M_{Z'} \gg \sqrt{s}$, we reach a better sensitivity in Møller scattering, where, again, an assumed 90% polarization makes a decisive difference.

More dramatic effects can be expected from dilepton (more recently renamed BIlepton) gauge bosons (with two units of charge and lepton number), such as P. Frampton has been proposing in his 331 model—which has the elegant implication of motivating the three-generation structure of the basic fermions in terms of a "natural" triangle anomaly cancellation [17]. It turns out that such states might come naturally in SU(15) grand unifying groups; with narrow widths, they would certainly lead to spectacular signals as s-channel peaks decaying into back-to-back high-transverse-momentum like-sign lepton pairs (Fig. 18).

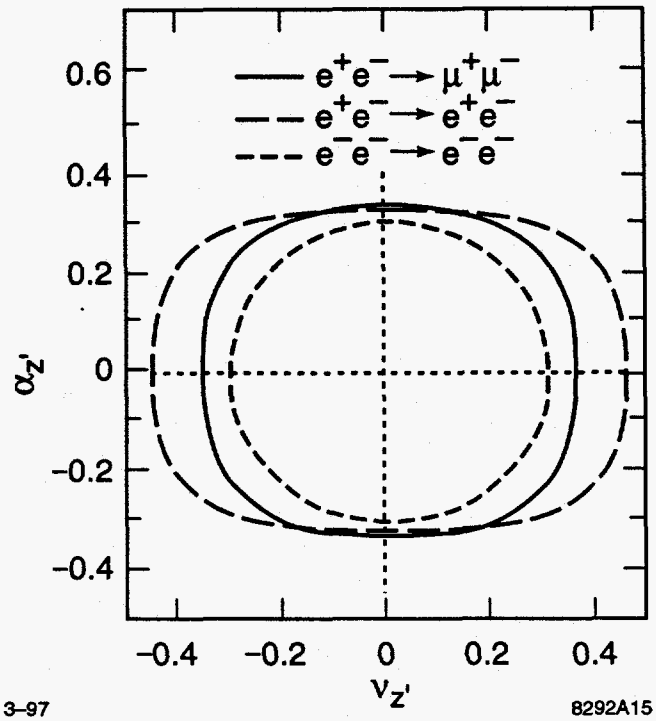

FIGURE 17. Contours of observability of Z' coupling to a Z' of 2 TeV mass.

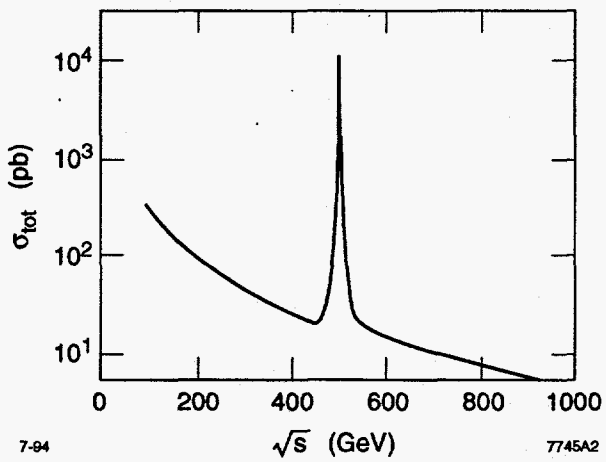

FIGURE 18. Production cross-section, as a function of energy, of dilepton gauge bosons in e^-e^- collisions. The 500 GeV mass and narrow width were assumed for illustration purposes.

H Heavy Majorana Neutrinos

One of the most tantalizing capabilities of our next Electron-Electron Collider's is quite unique, and will not easily be intruded upon by other machines: should neutrinos have Majorana mass terms, and should there be heavy (TeV-level) neutrino isosinglet states—as comes naturally in $E(6) \to SO(10) \to \ldots$ decompositions [18], a TeV e^-e^- collider might well provide spectacular signals for the process

$$e_L^- e_L^- \to W_{\rm long}^-, W_{\rm long}^- . \tag{9}$$

Unmistakable final-state signatures such as two unaccompanied high-p_T, like-sign leptons or two back-to-back jets that reconstruct to W masses, will be easily separated from backgrounds—and may therefore contribute to the resolution of two of the Standard Model's completely unexplained conundrums: the (SM-sanctioned) masslessness of neutrinos—through appropriate mass mixings—and the (presently absent) definition of the proper field operators for our neutral lepton sector.

The relevant scenario has been elaborated by Heusch and Minkowski [19], including the compatibility of a possible detection with present limits on the observation of neutrinoless nuclear double beta decay [20]. Again, cross-sections

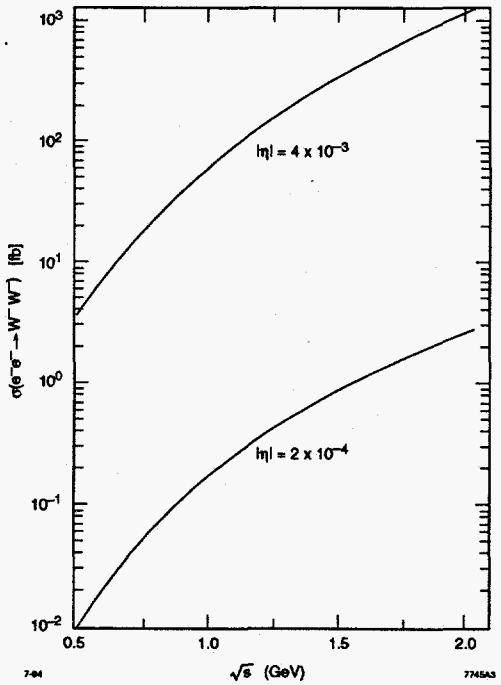

FIGURE 19. Energy dependence of the cross-section for the process $e^-e^- \to W_L^- W_L^-$ in the energy range of an NLC-type machine of a typical luminosity 10–100 fb^{-1}, for the range of neutrino mass matrix choices discussed in Ref. [18].

are detectably large only in one helicity combination; this means that even a few characteristic events will be able to establish an effect: a helicity flip in the incoming e^-e^- channel will have to eliminate the entire signal.

Obviously, the possible existence—well above any mass level that would have lent itself to direct observation—of Majorana neutrinos, will have to be examined in the framework of rare decays they might help mediate. The ensuing range of possible cross-sections for our process is shown in Fig. 19, as a function of collider energy [21]. A thorough examination of competing backgrounds [22] including only the hadronic decays of final-state W's is shown in Fig. 20. With anticipated collider luminosities, this energy range will fairly ensure detection within the first year of e^-e^- operation.

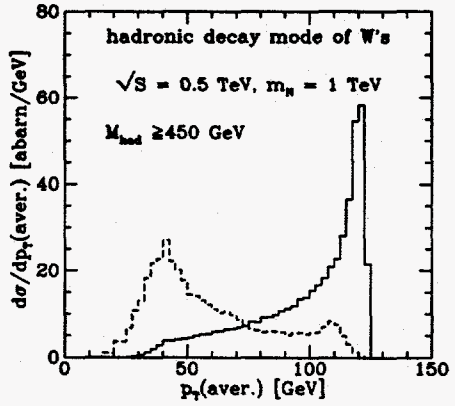

FIGURE 20. Signal (solid line) and background (dashed line) as a function of the average transverse momentum $p_\perp(aver.)$ of the jets. The hadronic invariant mass is required to be $m_{had} \geq 450$ GeV and the other parameters are chosen to be $\sqrt{s} = 500$ GeV, $m_N = 1$ TeV, $U^2_{eN} = 4 \times 10^{-3}$ (Ref. [22]).

IV THE ELECTRON-ELECTRON COLLIDER AS A PARENT CONFIGURATION FOR ELECTRON-PHOTON AND PHOTON-PHOTON COLLISIONS

We mentioned in the introductory remarks that the Next Electron Collider will provide not only ee initial states at full energy and luminosity, but also $e\gamma$ and $\gamma\gamma$ collisions with somewhat commensurate parameters. To make this promise come true by means of the backscatter of TeraWatt-powered laser photons off the incident electrons, a number of difficult experimental and technical challenges will have to be mastered [23]. What concerns us in the present context is the need to have those laser photons scatter off highly polarized, fully accelerated electrons (or positrons).

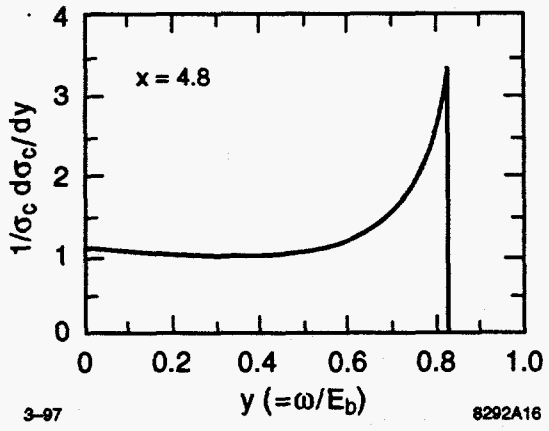

FIGURE 21. Spectrum of backscattered photons in the absence of electron polarization: an almost flat distribution for $y < 0.7$ builds up to a peak at the kinematic limit.

The motivation for this demand can easily be read off Figs. 21 and 22: Fig. 21 shows that the spectrum of the backscattered photons in the absence of electron polarization is essentially flat, with some moderate peaking at the upper end. This is clearly unacceptable as a kinematical definition of an "incoming beam." In Fig. 22(a), a fully polarized electron beam backscatters a like-helicity laser photon beam. The resulting backscattered like-helicity photon spectrum is very broad, and useless. Figure 22(b), on the other hand, has opposite-helicity laser photons backscatter off a fully polarized electron beam: a sharply peaked, highly polarized backscattered photon beam ensues, and only the small low-energy tail has the opposite polarization.

It is quite evident that there is no promise of useful photon-photon or electron-photon experimentation at the Electron Collider unless a high-quality e^-e^- version is implemented early on, and fully operational.

V CONCLUSION

As we are headed for a more closely defined proposal stage for the Next Electron Collider, it is incumbent on us to evaluate with the greatest care the physics potential of the collider configuration we believe to maximize its usefulness at unravelling the questions we will be facing some ten years from now. Given that the accelerator physics community will have no trouble whatever coming up with a design that permits us the choice of electron-electron and electron-positron initial states with comparable luminosities, identical energies, but differing helicity definitions, it is now time to scuttle the historical preoccupation with the annihilation diagram that has given us much of what the past decades taught us about the Standard Model and its signal successes. It is imperative that, in a fresh start, we take the trouble to consider what behooves us most on the exploratory trail *BEYOND* the Standard Model.

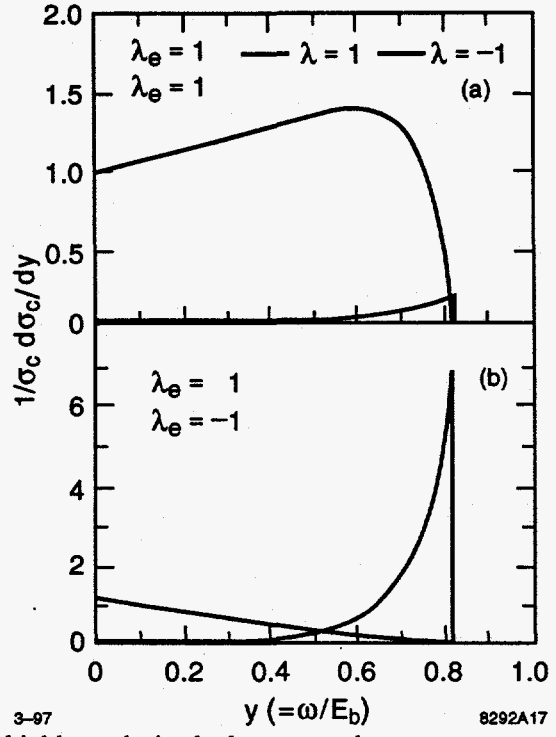

FIGURE 22. For highly polarized electrons, the spectrum and polarization of the backscattered photons is distinct. (a) For equal incident photon and electron helicities, the scattered photons have a broad distribution, and are highly polarized, retaining the incoming electron helicity. (b) For opposite incoming helicities, the spectrum is sharply peaked at the upper end, again with the incoming electron helicity. Only the broad low-energy tail has the opposite helicity.

TABLE 3. Additive quantum numbers of e^-e^- initial states.

	Q_{el}	s_z	L	L_e	I_3^W	Y^W
$e_L^-e_L^-$	-2	$1, 0, -1$	2	2	-1	-2
$e_L^-e_R^-$	-2	$1, 0, -1$	2	2	$-1/2$	-3
$e_R^-e_R^-$	-2	$1, 0, -1$	2	2	0	-4

As we do so, it is worth our while to look at the available quantum numbers of the initial state in the electron-electron configuration: Table 3 gives that information. The examples we chose above for an illustration of an e^-e^- physics program argue powerfully for a clean slate from which to choose among available incoming states when the time for decisions comes. Table 4 gives a possibly helpful overview of the principal topics we will want to attack once the new device is available some ten years hence: let us make sure our hardware—accelerator, interaction region(s), and detector(s) will permit us to make the most promising and comprehensive choice freely at that time.

TABLE 4. A listing of topics that will be investigated at a TeV-level linear collider. Check marks show the complementarity with which different initial states contribute prominently to their study. They also stake out unique contributions that the e^-e^- option will be able to make.

	QCD	$t\bar{t}$	H	SUSY	Strong WW	Anomalous Couplings	e^*	ν_M	Z'	X^{--}	Composite-ness
e^-e^-			√	√	√	√		√	√	√	√
e^-e^-	√	√	√	√	√	√			√		
$e^-\gamma$	√		√	√		√	√				
$\gamma\gamma$	√	√	√	√	√	√					

ACKNOWLEDGMENTS

I wish to thank the members of our international e^-e^- Working Group for their enthusiasm and steady encouragement. Tim Barklow and Michael Peskin helped me by discussing individual items. Nora Rogers and Lilian DePorcel deserve all credit for the preparation of this manuscript.

REFERENCES

1. For a historical account, see: B. Richter, in *Proceedings of the Third International Symposium on the History of Particle Physics* (Stanford University, Stanford, CA, 1992); SLAC-PUB-6023 (1992).
2. J. E. Spencer in e^-e^- '95, Int. J. Mod. Phys. **11**, 1675 (1996).
3. P. Chen *et al.*, in e^-e^- '95, Int. J. Mod. Phys. **11**, 1687 (1996); see also Ref. 2.
4. P. Minkowski, 1996 Snowmass, study to appear in *Proceedings of the 1996 DPF/DPB Summer Study on New Directions for High-Energy Physics* (Snowmass 96), (Snowmass, Colorado) 1997.
5. T. Rizzo, e^-e^- '95, Int. J. Mod. Phys. **11**, 1563 (1996).
6. H. Georgi, M. Machacek, Nucl. Phys. B **262**, 463 (1985).
7. F. Cuypers, G. J. van Oldenborgh, R. Rückl, Nucl. Phys. B **409**, 123 (1993)
8. M. Peskin, Lectures on Supersymmetry, Stanford University, CA (1997).
9. M. Chanowitz, LBL-PUB-32846 (1992).
10. V. Barger *et al.*, Phys. Rev. D **50**, 6704 (1994).
11. T. Han in e^-e^- '95, Int. J. Mod. Phys. **11**, 1541 (1996).
12. D. Choudhury, F. Cuypers, Nucl. Phys. B **429**, 33 (1994); Phys. Lett. B **325**, 500 (1994).
13. T. Barklow in e^-e^- '95, Int. J. Mod. Phys. **11**, 1579 (1996).
14. F. Cuypers, PSI, Villigen Report No. PSI-PR-96-09, 1996; Int. J. Mod. Phys. A **11**, 1571 (1996).
15. A. Leike, Z. Phys. C **62**, 265 (1994).
16. D. Choudhury, F. Cuypers, A. Leike, Phys. Lett. B **333**, 531 (1994).
17. P. H. Frampton and B. H. Lee, Phys. Rev. Lett. **64**, 619 (1990); P. H. Frampton, Phys. Rev. Lett. **69**, 2889 (1992).
18. P. Minkowski in *Proceedings of the Second Int. Workshop on Physics and Experiments with Linear* e^+e^- *Colliders*, (Waikoloa, HI, 1993), pp. 524-537.
19. C. A. Heusch and P. Minkowski, Nucl. Phys. B **416**, 3 (1994).
20. C. A. Heusch and P. Minkowski, Phys. Lett. B **374** 116, (1996).
21. C. A. Heusch, Nucl. Phys. B (Proc. Suppl.) **38**, 313 (1995).
22. C. Greub and P. Minkowski, DESY 96-253, BUTP 96128 (1996) to be published in *Proceedings of the 1996 DPF/DPB Summer Study on New Directions for High-Energy Physics* (Snowmass 96), (Snowmass, Colorado) 1997.
23. V. Telnov, Nucl. Instrum. and Methods A **355**, 3 (1995); and elsewhere in *Proceedings of the Workshop on Gamma-Gamma Colliders*; *ibid.* pp. 1-184.